International Journal of Applied Power Engineering (IJAPE)
Vol. 14, No. 4, December 2025, pp. 803~815
ISSN: 2252-8792, DOI: 10.11591/ijape.v14.i4.pp803-815

Design of a half-bridge inverter with digital SPWM control for pure sine wave output

Jalil Akaaboune, Bouazza El Mourabit, Mohamed Oulaaross, Mohamed Benchagra
Team Engineering and Applied Physics, Sultan Moulay Slimane University, Beni Mellal, Morocco

Article Info

Article history:

Received Feb 6, 2024
Revised Jun 24, 2025
Accepted Aug 3, 2025

Keywords:

Filter LC
Half-bridge
Harmonics reduction
Inverter control
MOSFETs
Power electronics
SPWM

ABSTRACT

To foster the widespread adoption of solar power, especially that produced by photovoltaic (PV) systems, we must move beyond the mere utilization of renewable energy sources. Prioritizing cost-effective approaches through innovative grid integration is essential. This strategic transformation significantly contributes to the global expansion of electrical energy production. One pioneering approach involves the implementation of inverters operating at high frequencies to efficiently filter and eliminate undesirable current harmonics, thus enhancing system performance. This innovative technique relies on the generation of rapid complementary digital pulse width modulation (PWM) signals, complete with built-in dead time, to manage a half-bridge inverter with a single phase. The paper recommends employing the IR2110 driver, an often-used component for MOSFET switch management, to execute this strategy. The entire system is controlled by high-frequency PWM signals, meticulously programmed for precision, generated by a microcontroller driver board. With its adaptability to various renewable energy conversion devices, this methodology extends its utility beyond solar energy. Practical tests have confirmed the efficacy of this strategy. Future research in this field should scrutinize the effect of PWM on system stability and harmonic distortion, explore advanced modulation methods, align PWM approaches with upcoming power electronics technologies, and work towards improving system efficiency.

Corresponding Author:

Jalil Akaaboune
Team Engineering and Applied Physics, Sultan Moulay Slimane University
Campus Mghilla, BP 523, 23000 Beni Mellal, Morocco
Email: jalil.akaaboune@gmail.com

1. INTRODUCTION

Global energy demand, projected to increase by 50% between 2018 and 2050, along with concerns over the environmental impact of fossil fuel consumption, has hastened the transition to sustainable energy sources such as solar, hydroelectric, and wind [1]. Fossil fuels, which continue to dominate the global energy sector, are a major source of carbon dioxide (CO2) emissions, playing a critical role in accelerating climate change and environmental degradation. In 2018, an estimated 89% of global CO2 emissions were attributed to the combustion of fossil fuels and industrial activities, underscoring their significant impact on the planet's ecological balance [2], [3].

The process of turning solar energy into electrical power is made possible by photovoltaic (PV) technology. PV systems need inverters to convert solar-generated direct current (DC) into alternating current (AC), which may be used effectively [4]. Beyond this essential conversion, inverters also play a role in optimizing system performance, monitoring output levels, and ensuring compliance with safety standards. PV systems have become a key element in the transition to clean energy. Over the past decade, global solar capacity has expanded significantly. In 2022, more than 200 GW of solar installations were added worldwide, with total installed solar capacity increasing by 203 GW that year [5]. This growth is driven by falling PV panel costs, technological advancements, and supportive policies [6].

To ensure the efficient use of solar energy, inverters play a crucial role in converting the DC generated by PV panels into AC, which is suitable for use in homes and on the grid. Modern inverter technologies achieve conversion efficiencies of up to 98%, significantly reducing energy losses during the conversion process [7]. However, solar energy generation is inherently intermittent, and inverters must be able to manage these fluctuations while maintaining a consistent AC output [8].

A key component in this transition is the inverter, an electronic device that transforms DC electricity generated by renewable sources like solar panels and wind turbines into AC electricity, suitable for households, businesses, and the power grid [9]. Inverters play a pivotal role in renewable energy systems, ensuring the compatibility of electricity generated by these sources with the existing electrical infrastructure. However, optimizing the efficiency, reliability, and cost-effectiveness of both renewable energy sources and inverters is crucial to making them more accessible to a wider range of users. Many renewable energy sources are intermittent, generating electricity at varying times, which presents challenges in ensuring a stable and reliable power supply [10]. Inverters must be meticulously designed to efficiently handle these varying input sources and provide a constant output of high-quality AC electricity [11], [12]. In essence, the challenge of harnessing renewable energy and the role of inverters are intertwined, working in harmony to establish a more sustainable and reliable energy system for the future. As technology advances and innovations emerge, continued progress can be expected in the development of renewable energy and inverter technologies. Inverters generate outputs that can be categorized into three distinct types according to their waveform: square wave, modified sine wave, and pure sine wave. The various waveforms are depicted in Figure 1. In terms of quality, pure sine wave inverters outperform other technologies, particularly with respect to total harmonic distortion (THD). Pure sine wave inverters exhibit significantly lower distortion levels, ensuring a higher quality of electrical power generation. Therefore, it is highly recommended to use pure sine wave inverters for solar panel applications to optimize both the efficiency and the quality of the electrical supply [13].

Among inverter control methods, pulse width modulation (PWM) is the most widely employed technique. The main goal of these modulation methods is to closely approximate sine waves, thereby improving the quality of the inverter output [14]. PWM, by shifting harmonics to frequencies at a higher level, facilitates efficient filtering. There are various types of modulation techniques, with the most recognizable ones including [15]: i) sinusoidal pulse width modulation, ii) modified pulse width modulation, iii) random pulse width modulation, iv) space vector modulation, and v) delta modulation.

The organization of the paper is as follows: Section 1 discusses the significance of renewable energy sources, with a particular focus on photovoltaic systems and the role of inverters. Section 2 discusses the design of the proposed high-frequency inverter system and its components, including the control circuit and power module. Section 3 details the characterization of the LC filter and the control methodology. Section 4 covers the simulation and experimental results, comparing the theoretical model with practical implementation. Finally, section 5 summarizes the study and proposes directions for future research.

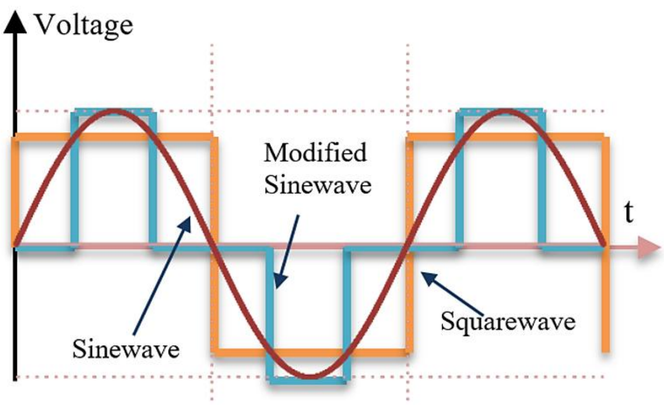

Figure 1. Various waveforms of an inverter

2. PROPOSED SYSTEM DESIGN AND CHARACTERIZATION

Figure 2 shows the schematic block diagram of the proposed system. It is made up of a control circuit based on a microcontroller that generates SPWM pulses. The inverter circuit will then supply the output. Finally, the sinusoidal signal was created by using an LC filter to reduce harmonics.

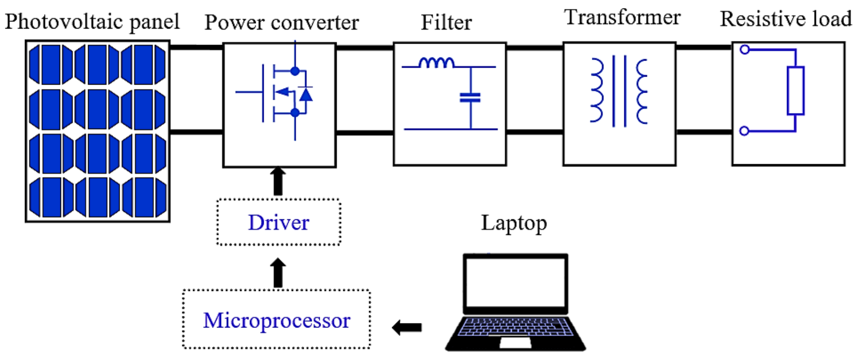

Figure 2. Schematic diagram of the entire circuit model

2.1. Power circuit module

The half-bridge configuration, fundamental to the implementation of the inverter, consists of two switches, S1 and S2 [16]. These switches within the same arm are designed to function in a complementary manner. This indicates that, as shown in Figure 3, one switch conducts electricity while the other concurrently blocks it. This configuration generates an output voltage waveform, as illustrated in Figure 4, which represents the inverter's output voltage.

Table 1 shows the switch combinations that are allowed for the inverter's half-bridge circuit. It also lists the switch combinations that are not allowed because they could cause a short circuit in the power supply. Table 1 has more information.

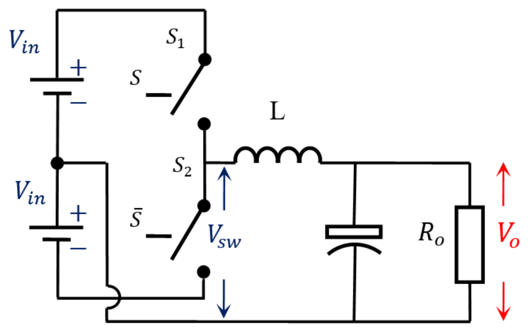

Figure 3. The half-bridge topology circuit

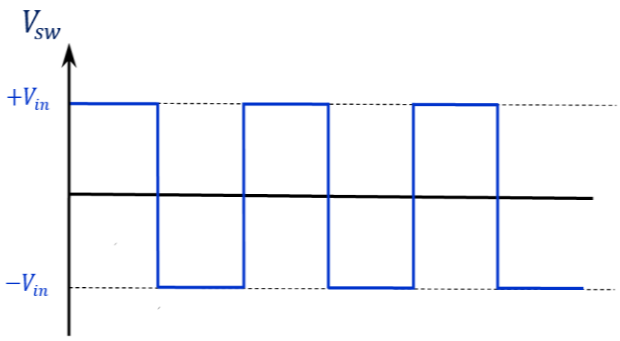

Figure 4. The voltage across the load

Table 1. Table of switch status [17]

S_1	S_2	Output voltage amplitude V_{Sw}
Off	Off	Voltage value of $V_{Sw} = 0$
Off	On	Voltage value of $V_{Sw} = -V_{in}$
On	Off	Voltage value of $V_{Sw} = +V_{in}$
On	On	The load is shorted

2.2. LC filter

To minimize THD, the filter design involves calculating the resonance frequency f_r for each switching frequency. A standard method is used to determine the inductance L and capacitance C values, as defined by (1).

$$f_r = \frac{f_{r_{Max}} + f_{r_{min}}}{2} = \frac{1}{2\pi\sqrt{LC}} \tag{1}$$

Where $f_{r_{min}} = 10\ f_m$ and $f_{r_{Max}} = 0{,}5\ f_{sw}$. The output voltage frequency, denoted by f_m, is 50 Hz and f_{sw} is the frequency of switching [18].

2.3. Control circuit module

Fully controllable semiconductor switches with the ability to turn on and off, such as BJT, MOSFET, or IGBT, must be selected in order to finish the project. The microcontroller utilized is an AT-Mega328, an 8-bit member of the AVR family [19]. The on and off states of the semiconductor switches T1 and T2 will be controlled by the microcontroller, which will be programmed to produce complementary PWM signals named HO and LO [20].

2.4. Gate driver

The IR2110 is a high-speed, high-voltage MOSFET driver that features separate and complementary output channels referenced to both the high-side (HO) and low-side (LO) of the circuit [21]. This complementary configuration prevents cross-conduction between switching devices and enables reliable and efficient control of power transistors, which explains the wide adoption of the IR2110 in power electronics applications. The device can operate with high-side voltages up to 500 V, low-side voltages up to 20 V, and supports logic inputs from 3.3 V to 15 V. Its output stages provide peak source and sink currents of up to 2 A, while propagation delays are matched to approximately 200 ns, ensuring accurate and stable transistor switching. Consequently, the IR2110 is particularly suitable for applications such as sinusoidal pulse width modulation (SPWM) generation, where speed, robustness, and numerical specifications guarantee precise and safe transistor operation.

3. THE PWM MODE FOR THE AVR PHASE AND FREQUENCY CORRECT

Digital pulse width modulation (DPWM) is an inverter control technique that employs a microcontroller to generate command signals. This approach enables precise adjustment of the switching frequency and pulse widths, thereby enhancing the quality of the generated power and effectively reducing harmonic distortions. It is particularly suitable for applications requiring fine regulation of voltage and frequency, such as solar inverters and power converters. The microcontroller implements a phase- and frequency-correct PWM mode based on a dual-slope counter. In this mode, the counter increments from a minimum value (BOTTOM) to a maximum value (TOP), and then decrements from TOP back to BOTTOM. The PWM waveform is generated by toggling the output compare channels OCnA and OCnB according to the values stored in the output compare registers (OCRnA and OCRnB). Each time the counter reaches the value defined in one of the OCR registers, the corresponding output channel changes its state (HIGH or LOW). In the inverted mode, the signal behaves oppositely, with the output compare channels switching with reversed polarity relative to the standard mode. The timing of the signal can be precisely controlled by adjusting the values in the compare registers, which determine the exact moments at which the channels toggle. Figure 5 illustrates this process, showing how the output channels OCnA and OCnB change states when the counter value matches the values in the compare registers, for both non-inverted and inverted modes.

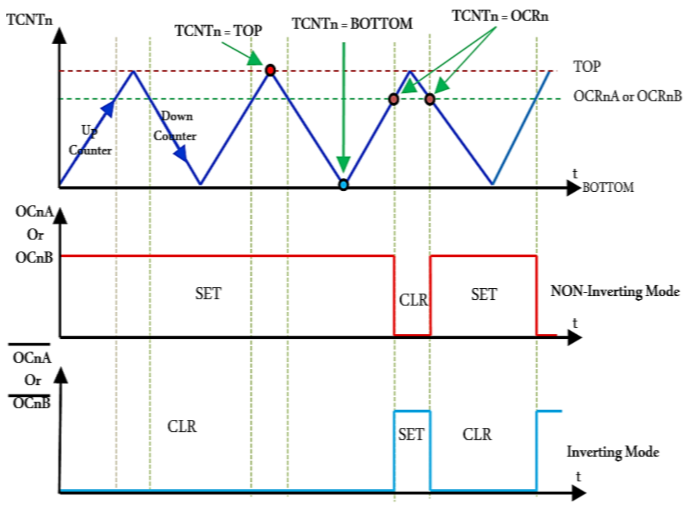

Figure 5. Diagram of the PFCPWM mode

This mode ensures a high degree of accuracy in the generated PWM signal, making it ideal for applications such as motor control, signal modulation, and other systems requiring precise frequency and duty cycle control. The following formula can be used to calculate the ICR1 (TOP) register's value in order to produce a 10 kHz PWM signal using a timer with a 16 MHz clock and a pre-scaler (N) of 1:

$$TOP(ICR1) = \frac{f_{clock}}{2 \times N \times f_{pwm}} = \frac{16\ \text{MHZ}}{2 \times 1 \times 10\text{Khz}} = 800 \quad (2)$$

where f_{clock} : timer clock frequency (16 MHz), N: prescaler value, and f_{PWM} : desired PWM frequency (10 kHz). Since each pulse is produced at a carrier frequency of 10 kHz every 100 microseconds, the pulse width needs to be modified at 100-microsecond intervals. The pulse width values for n, which range from 0 to 99, were computed using a spreadsheet.

$$Num = 800 \times sin\ (2 \times 180 \times n/200) \quad (3)$$

Normalizing the SPWM value to that is the next step, so:

SPWM [0] = 0 × 800 ⇒Num [0] = 0,
SPWM [1] = 0.03125 × 800 ⇒ Num [1] = 25,
SPWM [2] = 0.0625 × 800 ⇒ Num [2] = 50.

The difference in values between OCR1A and OCR1B creates two PWM signals with different pulse widths. By selecting the inverse mode for OCR1B, the two signals become complementary, with a dead time inserted between their transitions. This dead time ensures that neither signal is active simultaneously, preventing short circuits and protecting the circuit. The operation is illustrated in Figure 6.

After being modified by the modulation index value and the additional dead time, the value in table [Num] is read and input into the OCR1X register in the ISR. The dead time pulse width of 500 nanoseconds (t_d = 8 x 62.5 nS = 500 nS) is represented by the value of Δx = 8. At the moment, the modulation index is fixed at a value of 0.7.

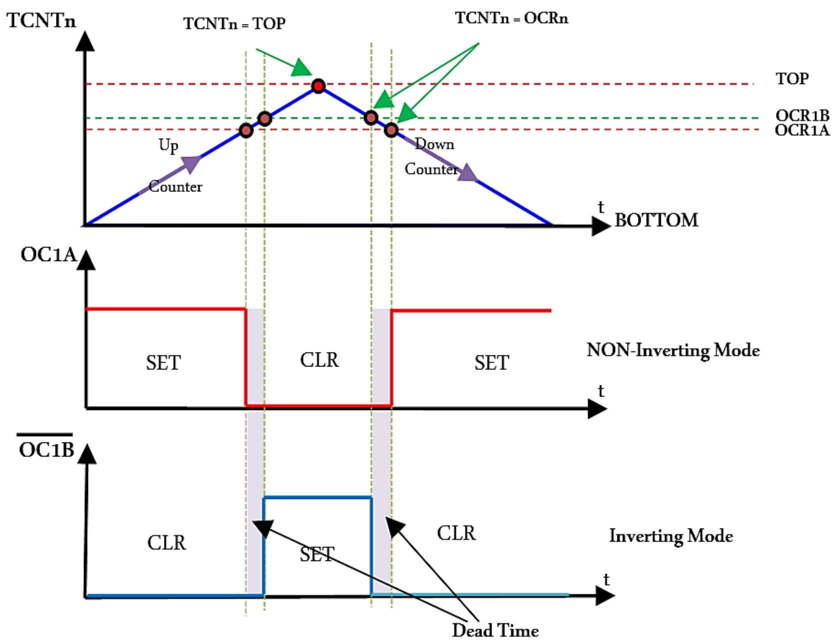

Figure 6. Dead time observation timing diagram

4. THE SIMULATION AND EXPERIMENTAL RESULTS

4.1. Deadtime-developed bipolar PWM waveforms

Figure 7 illustrates how a control model with dead time is used in the MATLAB/Simulink simulation of a single-phase half-bridge inverter using two MOSFETs. With a dead time of 500 ns, this model produces two complementary signals [22]. According to the IEC standard, the goal is to visualize the output signals and lower the THD to less than 5% [23]. The single-phase bipolar half-bridge inverter model is shown in Figure 8, where a PWM signal is produced by comparing a triangular carrier wave and a sinusoidal modulation signal. Table 2 summarizes the key system parameters, including input voltage, switching frequency, dead time, modulation index, and LC filter values used in this study.

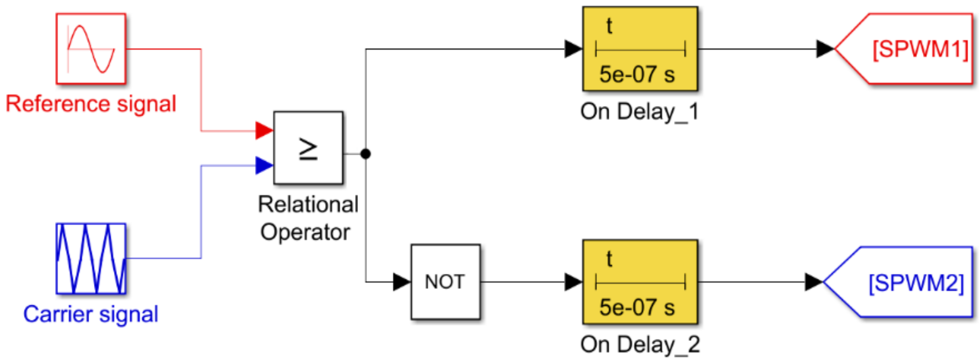

Figure 7. MATLAB Simulink simulation model of a control circuit with dead time

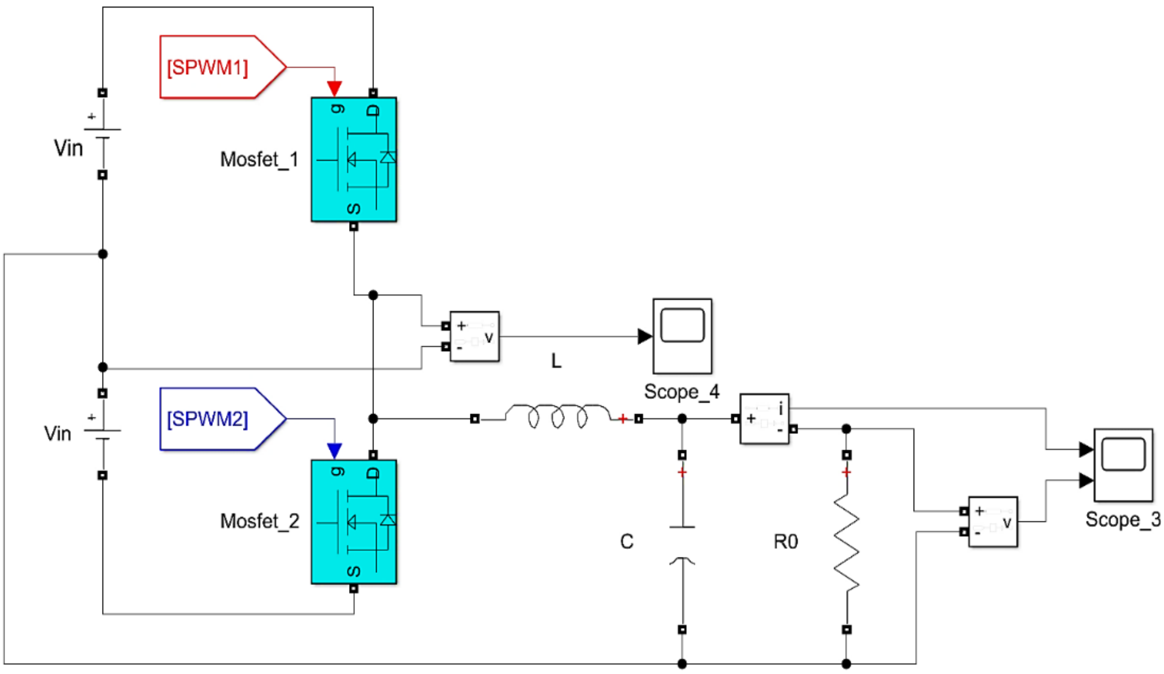

Figure 8. The simulation model for a single-phase bipolar half-bridge inverter

Table 2. Parameters for the system and control

Parameter	Symbol	Value
Voltage of DC Input	V_{in}	10 V
Switching frequency	f_{sw}	10 kHz
Dead time	t_d	500 ns
Modulation index	m	0.7
Filter inductance	L	10 mH
Filter capacitance	C	330 μF
Load resistance	R_0	10 Ω

To successfully avoid the shoot-through issue in semiconductor devices, like power metal-oxide-semiconductor field-effect transistors (MOSFETs), utilized in the motor's phase leg, a dead-time zone must be implemented [24]; however, the nonlinearity associated with the dead-time effect can cause distortions in voltage and current waveforms and generate high-order harmonics, significantly degrading motor performance, particularly at low speeds and under light-load conditions [25].

Figure 9 illustrates the dead time required to ensure proper operation of the switches. By introducing this interval, the SPWM waveform generator produces two complementary signals with dead time, allowing the switches to be safely turned on or off without causing a short circuit, while Figure 10 shows the resulting PWM output generated under these conditions, reflecting the influence of the implemented dead time on the waveform.

The simulation results obtained from MATLAB/Simulink show that the single-phase inverter produces an output voltage signal resembling that generated by the microcontrollers, with a voltage amplitude of 10 V and a switching frequency of 10 kHz. Figure 11 presents the voltage waveform at the inverter output before filtering, highlighting the inherent switching behavior of the PWM control. After applying the LC filter, the resulting pure sine voltage is shown in Figure 12, which also confirms that the maximum harmonic distortion of the nominal current remains within the 5% limit. For reference, the THD is defined as (4) [26].

$$THD_i = \frac{\sqrt{\sum_{h=2}^{n}(I_h)^2}}{I_1} \times 100 \quad (4)$$

Where I_h represents the current of the hhh-th harmonic and I_1 is the fundamental current.

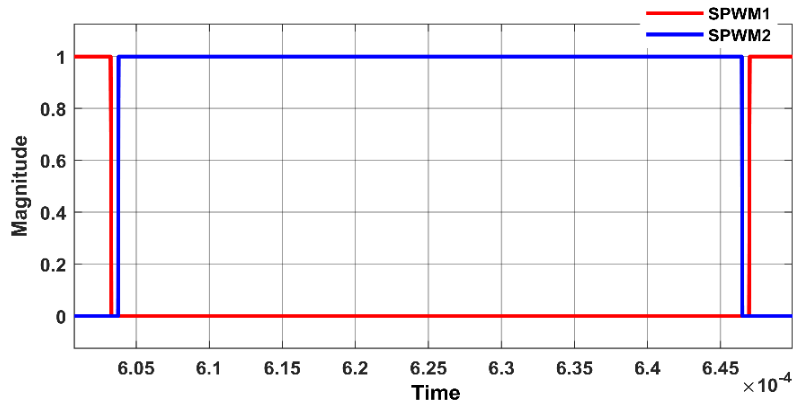

Figure 9. Impact of dead time on the voltage

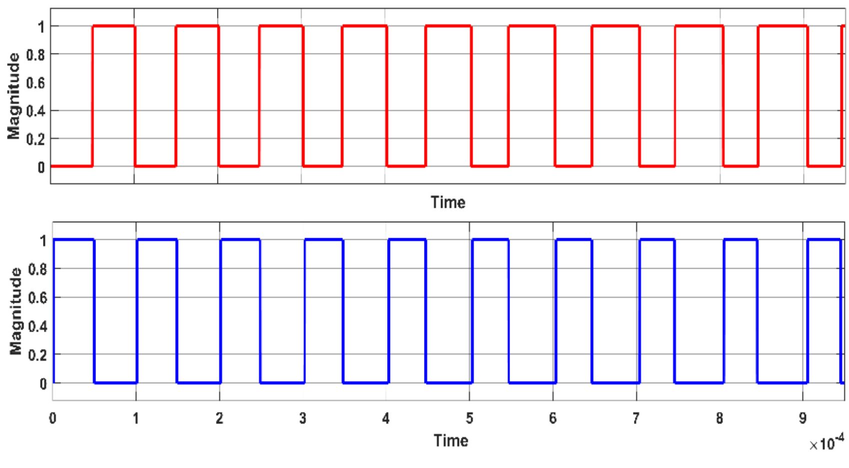

Figure 10. Complementary signal outputs

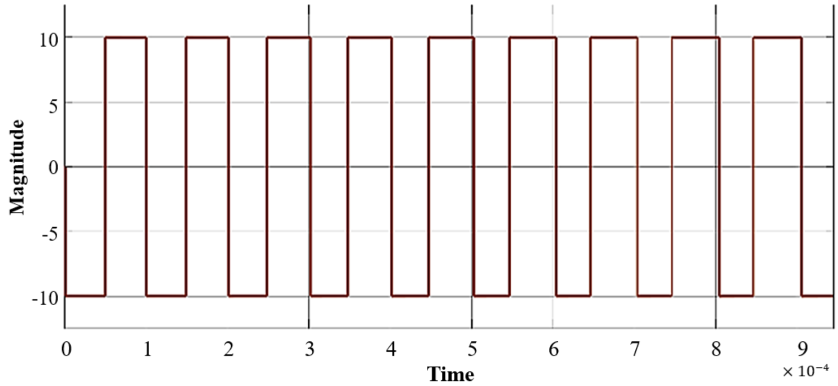

Figure 11. Voltage of the inverter's output

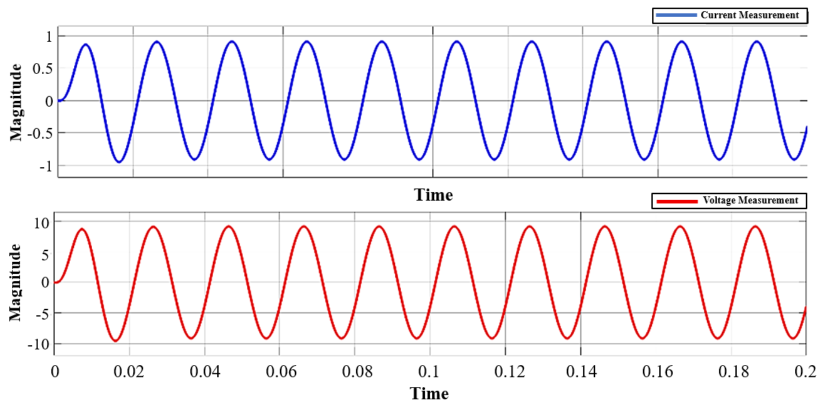

Figure 12. Pure sine voltage after LC filter

Figure 13 presents the output voltage waveform of the inverter before the application of the LC filter, highlighting the high harmonic content and waveform distortion. The THD significantly decreases after applying the LC filter, demonstrating its effectiveness in improving output signal quality. The fundamental voltage increases from 7 V to 9.114 V, while the THD drops from 174.35% to 0.19%, as illustrated in Figure 14. This reduction in THD indicates a cleaner output waveform, which closely resembles a pure sine wave, essential for enhancing the performance of power electronic systems. Additionally, a high switching frequency (f_{sw}) of 10 kHz helps reduce the size of the filter components and enhances the system's responsiveness and stability. These improvements are crucial for optimizing the efficiency of power electronic systems, ensuring more efficient operation and better power quality.

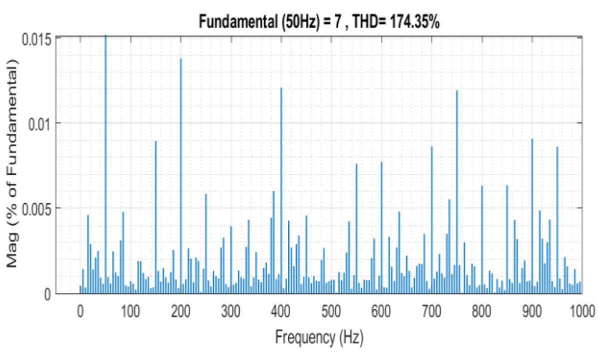

Figure 13. Bipolar inverter frequency analysis (absent a filter circuit)

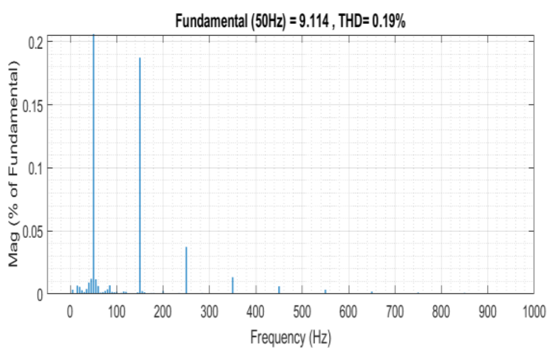

Figure 14. Bipolar inverter frequency analysis (using a filter circuit)

4.2. Result and discussion

As the initial step in the process, an ATmega328 board generates the control signals, which are subsequently injected into the pilot circuit. Figure 15 depicts the experimental prototype used in the study, while Figure 16 shows the practical circuit assembled on a protoboard and tested without an LC filter, serving as the preliminary setup for the experiments. A dual-channel digital oscilloscope was employed to observe the control signals, voltage waveforms, charging voltage, and condenser waveform.

Indeed, given that a switching device possesses a finite switching time, it is imperative to consider a dead time in the trigger signals generated by the Pulse-Width Modulation (PWM) in order to prevent the simultaneous triggering of two complementary switches within a single arm. Figure 17 presents the simulated gate driver signals of the inverter, clearly showing the applied dead time between the complementary pulses. Consequently, as evident in Figure 18, a 500 ns offset is observed as intended.

A clear correlation between the outcomes of the MATLAB simulation and their actual application can be seen in the figures that are displayed. The single-phase inverter prototype's measured output voltage waveform under a resistive load is shown in Figure 19, demonstrating the efficacy of the control strategy that was used. The output voltage waveform of a single-phase inverter with a resistive load is displayed in Figure 20. The waveform is a pure sine wave with a frequency of 50 Hz and a very low THD.

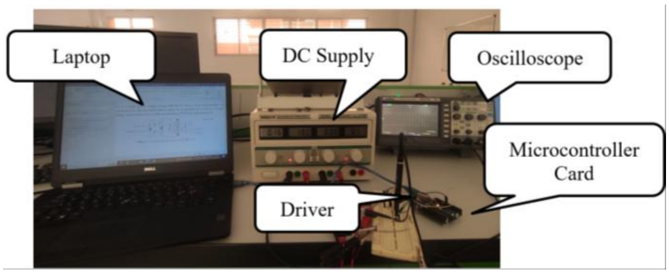

Figure 15. Experimental setup

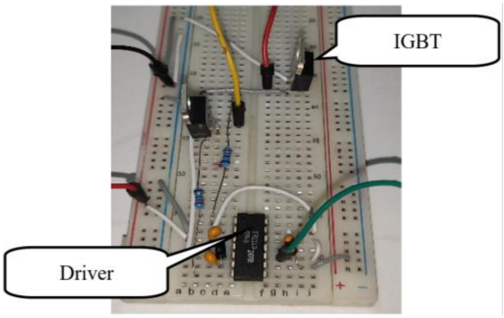

Figure 16. Without an LC filter, the practical circuit was run on a protoboard

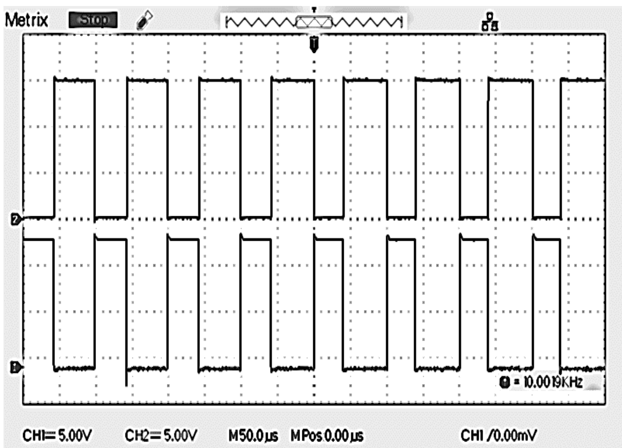

Figure 17. The IR2110 driver produces complementary signals at a frequency of 10 kHz

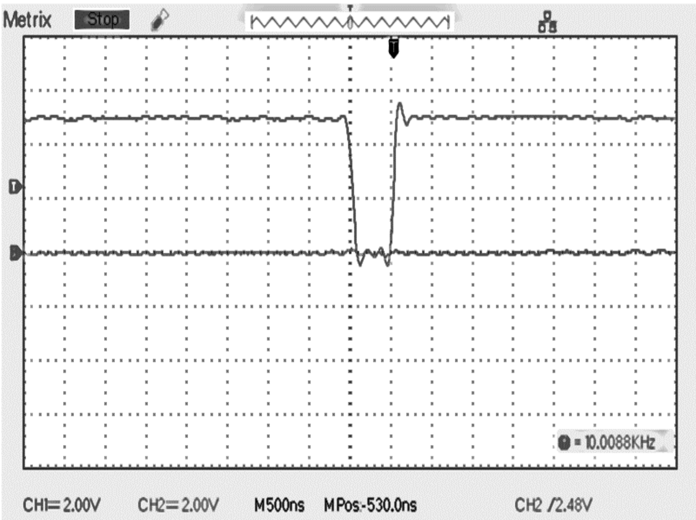

Figure 18. Dead time's effects on the microcontroller's voltage output

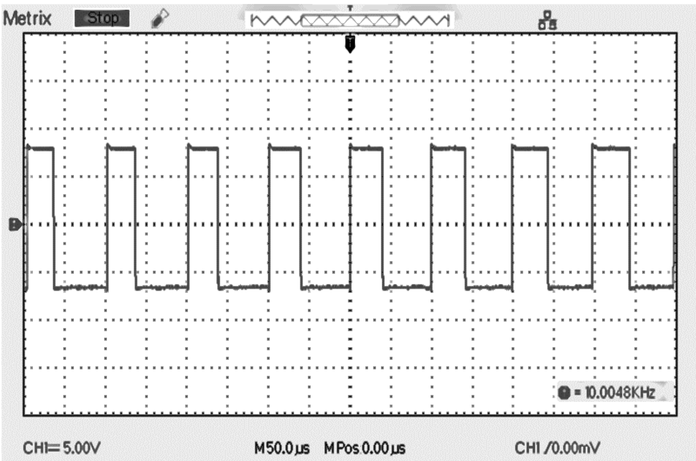

Figure 19. Output voltage of the inverter

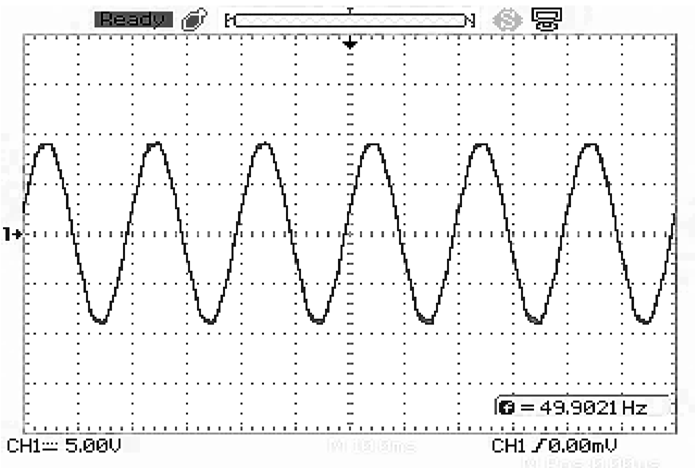

Figure 20. Sine wave after filter

5. CONCLUSION

The main objective of this study is to use a microcontroller to design a single-phase half-bridge inverter system. The experimental results are consistent with the outcomes of MATLAB/SIMULINK simulations. Thanks to the controller board, the inverter system is able to reach an output frequency of 50 Hz while achieving a THD of the voltage of less than 4%. The control method for the inverter switches is based on the sinusoidal pulse width modulation technique. However, the use of digital SPWM (DSPWM) via a microcontroller offers significant advantages over traditional analog SPWM, including greater flexibility, improved control accuracy, and reduced losses. The control circuit, developed using the AT-MEGA 328 microcontroller, also reduces the inverter's control hardware in terms of size, weight, and cost. Furthermore, applying a microcontroller allows easy changes to frequency/amplitude modulation ratios, dead time, and duty cycle through programming, without requiring any hardware modifications. The proposed inverter system is particularly well-suited for solar panel inverter applications in domestic settings. This version highlights the benefits of digital SPWM over analog SPWM, emphasizing its flexibility and efficiency improvements.

FUNDING INFORMATION

This research was self-funded by the authors. No external funding was received for the development of this work.

AUTHOR CONTRIBUTIONS STATEMENT

This journal uses the Contributor Roles Taxonomy (CRediT) to recognize individual author contributions, reduce authorship disputes, and facilitate collaboration.

Name of Author	C	M	So	Va	Fo	I	R	D	O	E	Vi	Su	P	Fu
Jalil Akaaboune	✓	✓	✓	✓	✓	✓	✓	✓	✓	✓	✓	✓	✓	✓
Bouazza El Mourabit	✓	✓	✓	✓	✓	✓	✓	✓	✓	✓	✓		✓	
Mohamed Oulaaross	✓	✓		✓	✓	✓	✓	✓	✓	✓	✓		✓	
Mohamed Benchagra	✓	✓	✓	✓	✓	✓	✓	✓	✓	✓	✓	✓	✓	✓

C : **C**onceptualization
M : **M**ethodology
So : **So**ftware
Va : **Va**lidation
Fo : **Fo**rmal analysis
I : **I**nvestigation
R : **R**esources
D : **D**ata Curation
O : Writing - **O**riginal Draft
E : Writing - Review & **E**diting
Vi : **Vi**sualization
Su : **Su**pervision
P : **P**roject administration
Fu : **Fu**nding acquisition

CONFLICT OF INTEREST STATEMENT

The authors declare that they have no known competing financial interests or personal relationships that could have appeared to influence the work reported in this paper.

DATA AVAILABILITY

The datasets used and/or analyzed during the current study available from the corresponding author, [AJ], on reasonable requests.

REFERENCES

[1] J. L. Holechek, H. M. E. Geli, M. N. Sawalhah, and R. Valdez, "A global assessment: can renewable energy replace fossil fuels by 2050?," *Sustainability*, vol. 14, no. 8, p. 4792, Apr. 2022, doi: 10.3390/su14084792.

[2] Global Climate and Health Alliance, *Cradle to grave: the health harms of fossil fuel dependence and the case for a just phase-out*, Jul. 2022. [Online]. Available: https://climateandhealthalliance.org/wp-content/uploads/2022/07/Cradle-To-Grave-Fossil-Fuels-Brief.pdf (Accessed: Apr. 25, 2024).

[3] J. Wang and W. Azam, "Natural resource scarcity, fossil fuel energy consumption, and total greenhouse gas emissions in top emitting countries," *Geoscience Frontiers*, vol. 15, no. 2, p. 101757, Mar. 2024, doi: 10.1016/j.gsf.2023.101757.

[4] R. M. Abdulhakeem, A. Kircay, and R. K. Antar, "Renewable power energy management for single and three-phase inverters design," *Energy Reports*, vol. 12, pp. 3096–3113, Dec. 2024, doi: 10.1016/j.egyr.2024.08.085.

[5] G. T. Chala and S. M. Al Alshaikh, "Solar photovoltaic energy as a promising enhanced share of clean energy sources in the future—a comprehensive review," *Energies*, vol. 16, no. 24, 2023, doi: 10.3390/en16247919.

[6] S. S. Panagoda *et al.*, "Advancements in photovoltaic (PV) technology for solar energy generation," *Journal Research Technology Engineering*, vol. 4, no. 3, pp. 30–72, 2023.

[7] L. T. Scarabelot, C. R. Rambo, and G. A. Rampinelli, "A relative power-based adaptive hybrid model for DC/AC average inverter efficiency of photovoltaics systems," *Renewable and Sustainable Energy Reviews*, vol. 92, pp. 470–477, 2018, doi: 10.1016/j.rser.2018.04.099.
[8] Q. Hassan, S. Algburi, A. Z. Sameen, H. M. Salman, and M. Jaszczur, "A review of hybrid renewable energy systems: solar and wind-powered solutions: challenges, opportunities, and policy implications," *Results in Engineering*, vol. 20, 2023, doi: 10.1016/j.rineng.2023.101621.
[9] A. Mikhaylov, "An overview of the roles of inverters and converters in microgrids," in *Unified Vision for a Sustainable Future: A Multidisciplinary Approach Towards the Sustainable Development Goals*, Springer Nature, 2024, pp. 69–85, doi: 10.1007/978-3-031-53574-1_3.
[10] H. Zsiborács *et al*., "Intermittent renewable energy sources: the role of energy storage in the European power system of 2040," *Electronics*, vol. 8, no. 7, Jul. 2019, doi: 10.3390/electronics8070729.
[11] R. Shriwastava, S. Gosavi, S. S. Khule, S. Hadpe, and M. P. Thakare, "A novel PWM technique for reduced switch count multilevel inverter in renewable power applications," *International Journal of Applied Power Engineering*, vol. 12, no. 1, pp. 1–12, 2023, doi: 10.11591/ijape.v12.i1.pp1-12.
[12] E. A. Etukudoh, A. Fabuyide, K. I. Ibekwe, S. Sonko, and V. I. Ilojianya, "Electrical engineering in renewable energy systems: a review of design and integration challenges," *Engineering Science & Technology Journal*, vol. 5, no. 1, pp. 231–244, 2024, doi: 10.51594/estj.v5i1.746.
[13] R. Mustikasari, M. J. Shubhi, L. Gumilar, S. Sujito, and A. Aripriharta, "Inverter performance comparison on solar panel applications," *Circuit: Jurnal Ilmiah Pendidikan Teknik Elektro*, vol. 7, no. 2, p. 142, Aug. 2023, doi: 10.22373/crc.v7i2.17631.
[14] M. F. N. Tajuddin, N. H. Ghazali, I. Daut, and B. Ismail, "Implementation of dsp based spwm for single phase inverter," in *SPEEDAM 2010*, IEEE, Jun. 2010, pp. 1129–1134, doi: 10.1109/SPEEDAM.2010.5542156.
[15] M. Youssef, "Simulation and design of a single-phase inverter with digital PWM issued by an Arduino board," *International Journal of Engineering Research and*, vol. V9, no. 08, Aug. 2020, doi: 10.17577/IJERTV9IS080237.
[16] N. F. A. Hamid, M. A. A. Jalil, and N. S. S. Mohamed, "Design and simulation of single-phase inverter using SPWM unipolar technique," *Journal of Physics: Conference Series*, vol. 1432, no. 1, p. 012021, Jan. 2020, doi: 10.1088/1742-6596/1432/1/012021.
[17] H. Vahedi and K. Al-Haddad, "Half-bridge based multilevel inverter generating higher voltage and power," in *2013 IEEE Electrical Power & Energy Conference*, IEEE, Aug. 2013, pp. 1–6, doi: 10.1109/EPEC.2013.6802961.
[18] M. Cengiz and T. Duman, "Sliding mode control for a single-phase grid-connected h-bridge npc inverter with a symmetrical LCL filter," *Computers and Electrical Engineering*, vol. 117, p. 109298, Jul. 2024, doi: 10.1016/j.compeleceng.2024.109298.
[19] Atmel, "ATmega328P 8-bit AVR Microcontroller with 32K bytes in-system programmable flash," 2015. [Online]. Available: https://ww1.microchip.com/downloads/en/DeviceDoc/Atmel-7810-Automotive-Microcontrollers-ATmega328P_Datasheet.pdf (Accessed: Mar. 10, 2024).
[20] G. C. Diyoke, I. K. Onwuka, and O. Oputa, "Development of a single–phase h-bridge inverter based on microcontroller sinusoidal pulse-width modulation scheme for residential load applications," *UNIZIK Journal of Engineering and Applied Sciences*, pp. 89–98, 2023.
[21] S. J. Shangguan, "Single-phase sine wave frequency inverter power supply," *Journal of Physics: Conference Series*, vol. 1087, p. 042004, Sep. 2018, doi: 10.1088/1742-6596/1087/4/042004.
[22] A. Balikci, B. T. Azizoglu, E. Durbaba, and E. Akpinar, "Efficiency calculation of inverter for PV applications using MATLAB and spice," in *2017 International Conference on Optimization of Electrical and Electronic Equipment (OPTIM) & 2017 Intl Aegean Conference on Electrical Machines and Power Electronics (ACEMP)*, IEEE, May 2017, pp. 593–598, doi: 10.1109/OPTIM.2017.7975033.
[23] A. Arranz-Gimon, A. Zorita-Lamadrid, D. Morinigo-Sotelo, and O. Duque-Perez, "A review of total harmonic distortion factors for the measurement of harmonic and interharmonic pollution in modern power systems," *Energies*, vol. 14, no. 20, p. 6467, Oct. 2021, doi: 10.3390/en14206467.
[24] X. Liu, H. Li, Y. Wu, L. Wang, and S. Yin, "Dynamic dead-time compensation method based on switching characteristics of the MOSFET for PMSM drive system," *Electronics*, vol. 12, no. 23, Dec. 2023, doi: 10.3390/electronics12234855.
[25] L. Zhang, L. Ren, S. Bai, S. Sang, J. Huang, and X. Zhang, "Self-adaption dead-time Setting for the SiC MOSFET boost circuit in the synchronous working mode," *IEEE Access*, vol. 10, pp. 57718–57735, 2022, doi: 10.1109/ACCESS.2022.3179403.
[26] R. Gupta and K. Sahay, "Comparative analysis of THD for square-wave inverter at different conduction modes," *International Journal of Applied Power Engineering (IJAPE)*, vol. 12, no. 3, pp. 312–320, Jul. 2023, doi: 10.11591/ijape.v12.i3.pp312-320.

BIOGRAPHIES OF AUTHORS

Jalil Akaaboune is a dedicated researcher who obtained a master's degree specialized in renewable energies and energy systems (Ms-ERSE) from the Faculty of Sciences Ain Chok in Casablanca, Morocco, in 2019. Currently, he is pursuing doctoral studies at the Faculty of Sciences and Techniques at Sultan Moulay Slimane University in Beni Mellal, Morocco. His research interests span across diverse facets of power electronics, covering intelligent systems for effective energy management, the innovation of advanced topologies for power converters, the integration of intelligent control strategies for optimizing these converters, and the enhancement of energy storage solutions. His primary research focuses on artificial intelligence techniques, such as neural networks, fuzzy logic, genetic algorithms, particle swarm optimization, and the imperialist competitive algorithm. Additionally, he is involved in research areas related to the gravitational search algorithm, power quality improvement, and the development of proportional integral controllers. He can be contacted at email: jalil.akaaboune@gmail.com.

Bouazza El Mourabit currently holds a position as a part-time professor at the Electrical and Electronic Engineering Laboratory at Sultan Moulay Slimane University in Beni Mellal, Morocco. He completed his master's degree in electrical engineering at the Higher Normal School of Technical Education in Rabat, Morocco, in 2011. Presently, he is actively pursuing his doctoral studies at the Faculty of Science and Technology within Sultan Moulay Slimane University, also located in Beni Mellal, Morocco. Elmourabit is an esteemed member of the "Team Engineering & Applied Physics (EAP)" research group at Sultan Moulay Slimane University. As a dedicated student researcher, his areas of expertise include the integration of intelligent control strategies to optimize static converters in power electronics, the enhancement of power quality, the development of energy storage solutions for electric vehicles, and the optimization of control systems employing techniques like neural networks, fuzzy logic, and genetic algorithms. He can be contacted at email: elmourabit.bza@gmail.com.

Mohamed Oulaaross is a student researcher at the Faculty of Sciences and Technology of Beni Mellal, Sultane Moulay Slimane University in Applied Mathematics and Physics. His main research areas include optimization and management of renewable energy using artificial intelligence technologies, power quality, and proportional integral controller. He obtained his master's degree in renewable energies-materials at the Faculty of Sciences of Rabat, Mohamed V University, and his professional license in electrical engineering and renewable energies at the High School of Technology of Berrechid, Hassan 1 University. He can be contacted at email: m.oulaaross@usms.ma.

Mohamed Benchagra was born in Beni-Mellal, Morocco, in 1982. He received the Ph.D. degree from Mohamed V University, Rabat, Morocco, in 2013. He is currently an assistant professor at the Technology High School (EST), Sultan Moulay Slimane University, Morocco. His research interests are electric machines, power electronics, power systems, and renewable energy. Dr. Benchagra is a member of the IEEE. He can be contacted at email: m.benchagra@gmail.com.